*DSC MRI, parametric imaging,*
*phantom studies*

Jacek RUMIŃSKI[*],
Barbara BOBEK-BILLEWICZ[**]

# LIMITATIONS OF DSC-MRI FOR QUANTITATIVE BRAIN PERFUSION

Synthesis of quantitative parametric images in DSC-MRI is presented. Critical review of major limitations of the DSC-MRI method is discussed. It includes investigation of measurement procedures/conditions as well as parametric image synthesis methodology. Simulations, as well as phantom studies were used to verify theoretical limitations of the DSC-MRI. Especially, estimation of the contrast (Gd-DTPA) concentration by EPI measurements, the role of a phantom and its pipes orientation, influence of a bolus dispersion, bolus arrival time, and other signal parameters on an image quality. As a conclusion testing software package is proposed.

## 1. INTRODUCTION

Parametric imaging becomes more and more popular. This includes DSC-MRI [4], ASL MRI [18], dynamic PET/SPECT [3], dynamic active thermography [12], etc. Parametric images represent values of reconstructed parameters for assumed tissue/activity model. This extends the structural imaging towards functional imaging. Qualitative parametric imaging could be extremely useful technique; however quantitative imaging could be even more powerful, especially using the same modality as used for structural imaging. This is a reason why DSC-MRI is an active area of research in quantitative cerebral perfusion.

### 1.1. THEORY

In the DSC-MRI brain studies, after injection of a bolus of contrast agent (Gd-DTPA), a series of images are measured. This time-sequence data presents local voxel activity of contrast (blood) flow and distribution. It is assumed, that measured MRI signal values are proportional to the contrast concentration. Contrast concentration as a function of time is measured for brain supported arteries. This function can be estimated as the arterial input function (AIF). Assuming ideal conditions this function should be an ideal impulse function, so measuring the output function (impulse response) one can specify properties of the object under study, including mass flow, mass volume, and mean transfer time. Since AIF is not an

[*] Department of Biomedical Engineering, Gdansk University of Technology
[**] Department of Neuroradiology, Medical University of Gdansk

ideal impulse function (dispersion and delay) and because in DSC-MRI measurements are done from volume of interest (VOI), de-convolution should be used to calculate VOI impulse response [9]

$$C_t(t) = \frac{\rho}{Kh}\int_0^t C_a(\tau)\cdot\left(F\cdot R(t-\tau)\right)d\tau\,, \qquad (1)$$

where: $C_a(t)$ - contrast concentration in the artery (e.g., Middle Cerebral Artery) – Arterial Input Function AIF, $C_t(t)$ - contrast concentration in the tissue, $\frac{\rho}{Kh}$ - scaling factor (quantitative description) $\rho$ – mean tissue density of a brain, $\rho$=1,04 g/mol; *Kh* – hematocrit ration (large to small arteries) *Kh=(1-Hd)/(1-Hm); Hd=0.45*; *Hm=0.25*; *F*R(t)* – scaled impulse response (residue function) inside VOI, *R(t)* - represents fractional tissue concentration:

$$R(t) = 1 - H(t) = 1 - \int_0^t h(\tau)\cdot d\tau\,, \qquad (2)$$

Where: *h(t)* - transport function - impulse response (an ideal instantaneous unit bolus injection). Distribution of transit times through the voxel; depends on the vascular structure and flow. The model is based on tracer kinetics for non-diffusible tracers – contrast material remains intravascular [8].

Scaled impulse response could be calculated using Fourier transforms (*FFT*) or matrix algebra (with matrix decomposition *SVD* to eliminate singularities). Since *R(t=0)* should be equal to 1, then $F\cdot R(t=0) = F = CBF$ (Cerebral Blood Flow). Cerebral blood volume (proportional to the normalized total amount of tracer) can be calculated as

$$CBV = \int_0^\infty C_t(\tau)\cdot d\tau \;\Big/\; \frac{\rho}{Kh}\int_0^\infty C_a(\tau)\cdot d\tau\,, \qquad (3)$$

Based on central volume theorem, mean transit time (average time required for any given particle of tracer to pass through the tissue after an ideal bolus injection) can be estimated as

$$MTT = CBV/CBF. \qquad (4)$$

Three types of quantitative parametric images (CBF, CBV, MTT) synthesized under strictly controlled procedure, offer additional information for brain studies.

## 2. METHODOLOGY

Quantitative, parametric imaging requires understanding and analysing major limitations of the method. Conclusions of such a critical study may be used for quality assurance and control in parametric DSC-MRI imaging. Major limitations of the DSC-MRI are related to:

1. Sequence specification of the MRI study
2. DSC-MRI procedure
3. Tracer concentration measurement
4. Arterial Input Functions measurement
5. Image synthesis procedure

Ad. 1. Sequence specification of the MRI study

Perfusion imaging techniques use as well non-EPI (echo planar imaging) as EPI systems. However EPI systems are preferred because of superior performance [15]. Using EPI system it is usually possible to choose between gradient echoes (GE EPI) or spin echo (SE EPI). With GE EPI the SNR is higher than for SE EPI. Large arteries highly influence on measured signal (susceptibility contrast arises from large and small vessels), so also the AIF is more accurate. However, the local brain tissue should be evaluated, so small changes in local blood distribution are more visible using SE EPI [2]. SE technique reflects micro vascular perfusion and calculated CBV is limited only to micro vascular CBV. However SE signal is more influenced by the dispersion caused by vasculature [11], and parametric images quality could be unacceptable for quantitative imaging. In [14] authors concludes that results on SE EPI studies are proportional (linear relation) to those obtained with GE EPI, so SE and GE EPI are equally useful in clinical measurements.

Ad. 2 DSC-MRI procedures

DSC-MRI procedure uses bolus injection of a contrast agent. Two important properties are related: injection dose and injection speed. Higher injection dose (typical 0.1-0.2 mmol/kg b.w.) can increase sensitivity with the DSC MRI. However to high dose leads to signal drops below background noise level. Low injection speeds resulted in a broadening of the input function. This leads to broadening of the contrast passage through the brain tissue. Low injection speeds ( < 4 ml/s) produce underestimation of CBF. The same effect was observed for the temporal resolution [16]. High temporal resolution imaging is necessary, since the transit time of the bolus through the tissue is usually a few seconds.

Ad. 3. Tracer concentration measurement

MRI is not able to directly measure the tracer concentration. It must be measured indirectly through its effect on MRI signal intensity [5]. It is assumed that

$$C_c(t) = -\frac{1}{k \cdot TE} \ln\left(\frac{S_c(t)}{S_0}\right), \qquad (5)$$

where: $C_C(t)$ – tracer concentration in time, TE – echo time, $S_0$ - measured MR signal intensity without tracer, $S_c(t)$ - measured MR signal intensity after a bolus of contrast agent injection, k – proportionality constant.

Proportionality constant k depends on many parameters, including those which describe object properties (e.g., size/orientation of vessels), MRI pulse sequence, etc. In literature it is usually assumed, that k is constant for all analyzed voxels (e.g., k=1). This assumption is very practical, but it limits quantitative cerebral flow estimation. In [16] author introduced calibration procedure for estimation of the influence of the contrast (Gd-DTPA) concentration on the measured MR signal. However this calibration is limited for the presented set-up (e.g. dual echo GR-EPI).

Other limitations on quantitative tracer contrast calculation are related to: patient orientation (vessels) in reference to the magnetic field and gradient coils [15], partial volume effect [16], region of interest specification ROI, etc.

Ad. 4. Arterial Input Functions measurement

In quantitative DSC-MRI it is crucial to exactly measure an input function. Based on the AIF the required signal (F*R(t)) is deconvolved and used for quantitative maps synthesis. Theoretically the AIF describes concentration of contrast agent in the feeding vessel to the VOI. Practically it could be localized far away from VOI (carotid artery, middle cerebral artery). The path between measured AIF source and true AIF localization is unknown. It can introduce the AIF delay and dispersion [6]

$$C_a^{true}(t) = C_a(t) \otimes h(t) \tag{6}$$

Where: h(t) – vascular transport function, e.g.:

$$h(t) = \frac{1}{t_D} \cdot \exp\left(\frac{-t}{t_D}\right) \tag{7}$$

where: $t_D$ - dispersion constant.

The AIF delay and dispersion may be described by absolute parameters: D – dispersion described by Gauss distribution (standard deviation) in reference to the ideal impulse; $t_d$ - delay time, equal to MTT (mean transit time between measured and real AIF location) for no dispersion; in case of dispersion equal to

$$t_d = MTT \cdot \left(\frac{D_{MAX} - D}{D_{MAX}}\right), \tag{8}$$

Similar description was proposed in [16].

Another estimation of the AIF dispersion could be calculated by normalized the full width at half-maximum (FWHM) of the tissue concentration time curve to the FWHM of the AIF concentration time curve, measured from large artery [11].

Delay and dispersion introduce problems in perfusion quantification – significant underestimation of CBF and overestimation of MTT. Correction of delay error may be done using bolus arrival time information. Delays of 1 to 2 seconds can introduce an approximately 40% underestimation of CBF and 60% overestimation of MTT [6]. Another problem with the AIF determination is reproducibility. Some solutions introduce symmetry comparisons (left and right sides for AIF measurements), or automatic AIF estimation [8]. In [15] authors suggest that AIF ROI should be positioned near to a feeding cerebral artery (carotid artery, middle cerebral artery), as blood flow introduce signal enhancement.

Theoretically, the AIF improvements can be introduced increasing the injection dose. However, signal can drops below background noise level resulting in the AIF underestimation.

Ad. 5. Image synthesis procedure

Parametric image synthesis uses calculation of CBF, CBV and MTT values for pixel time series (typical procedure: sampling period: 1-2s; number of slices: 12; resolution 128x128). Extracted time series for each pixel represents $S_c(t)$ samples in (5). After $S_c(t)$ conversion to concentration time curve, de-convolution of R(t) is required for quantitative maps. Several methods have been proposed, divided in two categories: model dependent and model independent. In model dependent – vascular bed is modelled as one single, well-mixed compartment, using

$$R(t) = \exp(-\frac{t}{MTT}), \tag{9}$$

In model independent – CBF, R(t) are not assumed, but determined by nonparametric de-convolution (R(t) – unknown). Two main techniques are used: Fourier and SVD. Other techniques: de-convolution using orthogonal polynomials, where the AIF is approximated by a subset of an orthogonal function system [13]; analytical solution using maximum likelihood method (iterative algorithm) [17]; method using the Gaussian process for de-convolution [1].

Quantitative measurement requires elimination of recirculation contributions to the MR signal. It can be done with detection of the beginning of the recirculation phase (arbitrary cut) or fitting to an assumed model (curve – e.g. gamma variety functions) [7]. Absolute measurement of CBF can be also used assuming fixed values for the relevant proportionality constants (Kh, $\rho$, k) and cross-calibration with other techniques e.g. SPECT, CT, PET [10].

### 2.1. SIMULATIONS

Based on the introduced description of quantitative limitations of DSC-MRI different simulations were performed using Math lab code and Java prepared applications. The concentration signal was modelled as

$$C(t) = \begin{cases} K(t-t_0)^{\beta} \cdot e^{-\alpha(t-t_0)}, t > t_0 \\ 0, t \le t_0 \end{cases} ; \qquad (10)$$

Where: K, α, β model parameters (used β=3, α=2/3), $t_0$ - bolus arrival time (BAT).

Recirculation component was included in C(t) as a scaled Gaussian function shifted in time and exponential component (1-exp(-t/T)). Resulted AIF was then convolved with residue impulse response function R(t), described by (1). MTT was set form the <1s,10s> range, resulting in different C(t) for simulated tissues. Additional simulations were performed introducing additive noise for modelled MR signal $S_c(t)$

$$C_c(t) = -\frac{1}{k \cdot TE} \ln\left( \frac{S_c(t) + n(t)}{S_0} \right); \qquad (11)$$

Where n(t) – additive noise (Gaussian).

This was achieved by modelling C(t), then calculating $S_c(t)$, again calculation of C(t). Simulations were performed using different noise values, for FFT and SVD de-convolution.

### 2.2. PHANTOM STUDIES

Phantoms for static and dynamic measurements of contrast concentration were prepared. A set of glass (total volume 45ml) and plastic (total volume 30 ml) pipes (diameters: 2,5mm; 6mm, 9mm) was fixed in plastic bottles (2l and 5l) giving 5 different water phantoms (Fig. 1).

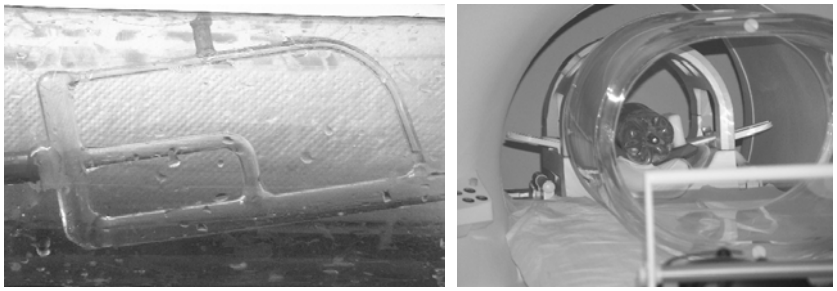

Fig. 1. Water phantom in the MR scanner.

Static measurements were performed for different contrast concentrations (10 different concentrations in the range of 0 mmol/l - 25mmol/l). Dynamic measurements were performed in presence of continuous water flow (10ml/s) and injection of contrast agent (Magnevist, Schering AG, Germany). SE-EPI was used with: 12 slices, 60 time samples, TR=1250-1610ms; TE=32=53ms; slice thickness 5-10 mm; 3 different localization of the phantom.

## 3. RESULTS

In simulations, increasing the noise the FFT de-convolution was much more sensitive than SVD. If the BAT of the real AIF (i.e., unknown AIF convolved with the VOI R(t)) is longer than BAT of the measured AIF (i.e., AIF used for de-convolution) then de-convolved R(t) is shifted in time. This is a result of the convolution operation property. Concluding, if AIF is delayed (keeping all other properties the same) calculated R(t) is only shifted in time, which not contribute (excluding shift) to CBF (see (3)). Broadening the C(t) resulted in inaccurate automatic BAT detection, and difficulties for a manual decision. Recirculation (simulated as shifted and scaled Gaussian function) and dispersion of AIF generates underestimation of F*R(t) amplitude. In case of recirculation however the underestimation is smaller than for the AIF dispersion (from (8) $t_D$=2->76%; $t_D$=4->56%; $t_D$=8->33%; linear relation e.g., y = -0,175x + 2,47).

Phantom studies results (fig. 2) can be concluded as:

- phantom orientation (pipes) in reference to the magnetic field and gradient coils did not introduce significant change in C(t) estimation;
- for low Gd concentration (<1.25 mmol/l) T1 enhancement was observed;
- flow introduce up to 10 % enhancement so AIF ROI should be positioned near to a feeding cerebral artery or it should be calibrated;
- for high concentration (>12.5 mmol/l) signal drops below background noise;
- there is a systematic error in $S_0$ estimation (even 10%),
- AIF ROI and slice thickness selection should be carefully controlled (underestimation of AIF).

## 4. DISCUSSION AND CONCLUSION

Synthesis of parametric, quantitative images with DSC-MRI should be carefully controlled which includes: measurement and post-processing. In the measurement phase calibrating phantom should be used, and in our opinion this is an important direction for further studies. In case of post-processing we prepared software (Java) which generates synthetic DICOM files for a simulated C(t) signals.

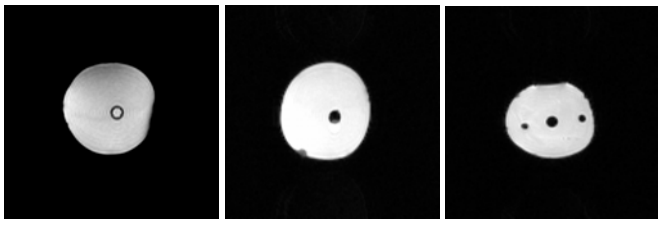

Fig. 2. Some results of phantom studies: from left – water in pipe (0mmol/l), contrast agent in the pipe (6.25mmol/l), contrast agent in dynamic study.

The software is based on the simulation model described in this work (eq. (1)-(11)) with possibility of parameters definition by a user. The user can define rectangles which indicate ROI with different parameters; the AIF rectangle is automatically generated in the user defined location. Resulted data could be used to validate qualitative perfusion post-processing software. Currently we investigate 6 different software packages and results we be published soon.

BIBLIOGRAPHY


[1] ANDERSEN I.K., SZYMKOWIAK A., RASMUSSEN C.E., HANSON L.G., MARSTRAND J.R., LARSSON H.B.W., HANSEN1 L.K., PERFUSION Quantification Using Gaussian Process Deconvolution, Magnetic Resonance in Medicine, 48:351–361, 2002.

[2] BOXERMAN JL, HAMBERG LM, ROSEN BR, WEISSKOFF RM. MR contrast due to intravascular magnetic susceptibility perturbations. *Magn. Reson. Med.* 34:555-66, 1995.

[3] CAI W., FENG D. D., FULTON R., Content based retrieval of dynamic PET functional images, IEEE Transactions on Information Technology in Biomedicine 4 (2)152-158, 2000.

[4] CALAMANTE F., GADIAN D.G., CONNELLY A., Quantification of Perfusion Using Bolus Tracking Magnetic Resonance Imaging in Stroke. Assumptions, Limitations, and Potential Implications for Clinical Use, *Stroke*.;33:1146-1151, 2002.

[5] CALAMANTE F, THOMAS D L, PELL G S, WIERSMA J and TURNER R Measuring cerebral blood flow using magnetic resonance imaging techniques *J. Cereb. Blood Flow Metab.* 19 701–35, 1999.

[6] CALAMANTE F, GADIAN D G and CONNELLY A 2000 Delay and dispersion effects in dynamic susceptibility contrast MRI: simulations using singular value decomposition *Magn. Reson. Med.* 44 466–73

[7] CHEONG L H, KOH T S, HOU Z, An automatic approach for estimating bolus arrival time in dynamic contrast MRI using piecewise continuous regression models Phys. Med. Biol. 48:N83–N88, 2003.

[8] MORRIS E.D., TASCIYAN T.A., VANMETER J.W., MAISONG J.M., ZEFFIRO T.A., Automated determination of the arterial input function for MR perfusion analysis. Available: www.indyrad.iupui.edu/public/emorris/Sensor/poster.pdf

[9] ØSTERGAARD L, Weisskoff R M, Chesler D A, Gyldensted C and Rosen B R High resolution measurement of cerebral blood flow using intravascular tracer bolus passages: I. Mathematical approach and statistical analysis, II. Experimental comparison and preliminary results *Magn. Reson. Med.* 36 715–36, 1996.

[10] ØSTERGAARD L, SMITH DF, VESTERGAARD-POULSEN P, HANSEN SB, GEE A, GJEDDE A, GYLDENSTED C. Absolute Cerebral Blood Flow and Blood Volume Measured by MRI Bolus Tracking: Comparison with PET Values. *J.Cereb.Blood Flow Metab.* 18:425-32, 1998.

[11] QUARLES, C.C., PATHAK, A.P., WARD, B.D., REBRO, K.J., SCHMAINDA, K.M. Reliability of Measuring Tumor Perfusion using Dynamic Susceptibility Contrast MRI: The Influence of Vascular Structure and Imaging Technique. 10th Scientific Meeting & Exhibition of the International Society for Magnetic Resonance in Medicine, Honululu, Hawai'i, USA, May 18-24, 2002.

[12] RUMIŃSKI J., KACZMAREK M., NOWAKOWSKI A., Medical Active Thermography – A New Image Reconstruction Method, Lecture Notes in Computer Science LNCS2124, Springer, 274-181, 2001.

[13] SCHREIBER WG, GÜCKEL F, STRITZKE P, SCHMIEDEK P, SCHWARTZ A, BRIX G, Cerebral blood flow and cerebrovascular reserve capacity: estimation by dynamic magnetic resonance imaging. *J Cereb Blood Flow Metab* 18:1143-1156, 1998.

[14] SIMONSEN C.Z., OSTERGAARD L., SMITH D.F., VASTERGAARD-PULSEN P., GYLDENSTED C., Comparision of gradient- and spin-echo imaging: CBF, CBV and MTT measurements by bolus tracking, Journal of Magnetic Resonance Imaging, 12:411-46, 2000.

[15] SORENSEN A.G., REIMER P., Cerebral MR Perfusion Imaging, Principles and Current Applications, Georg Thieme Verlag, Stuttgart, 2000.

[16] VAN OSCH T., Evaluation of cerebral hemodynamics by quantitative perfusion MRI, PhD thesis, Image Science Institute, Utrecht, 2002.

[17] VONKEN EP, BEEKMAN FJ, BAKKER CJ, VIERGEVER MA. Maximum likelihood estimation of cerebral blood flow in dynamic susceptibility contrast MRI. *Magn.Reson.Med.* 41:343-50,1999.

[18] WANG J., ALSOP D. C., Li L., LISTERUD J., GONZALEZ-At J. B., SCHNALL M. D., DETRE J. A., Comparison of Quantitative Perfusion Imaging Using Arterial Spin Labeling at 1.5 and 4.0 Tesla, Magnetic Resonance in Medicine 48:242–254, 2002.

This work was partly supported by the grant of Polish State Committee for Scientific Research (2003-2006) 4 T11E 042 25.